Proc. Natl. Acad. Sci. USA
Vol. 93, pp. 11510–11515, October 1996
Biochemistry

Increased histone H1 phosphorylation and relaxed chromatin structure in *Rb*-deficient fibroblasts

RAFAEL E. HERRERA*, FENG CHEN*†, AND ROBERT A. WEINBERG*†‡

*Whitehead Institute for Biomedical Research, 9 Cambridge Center, Cambridge, MA 02142; and †Department of Biology, Massachusetts Institute of Technology, Cambridge, MA 02139

Contributed by Robert A. Weinberg, August 2, 1996

ABSTRACT **Fibroblasts derived from embryos homozygous for a disruption of the retinoblastoma gene (*Rb*) exhibit a shorter G_1 than their wild-type counterparts, apparently due to highly elevated levels of cyclin E protein and deregulated cyclin-dependent kinase 2 (CDK2) activity. Here we demonstrate that the $Rb^{-/-}$ fibroblasts display higher levels of phosphorylated H1 throughout G_1 with the maximum being 10-fold higher than that of the $Rb^{+/+}$ fibroblasts. This profile of intracellular H1 phosphorylation corresponds with deregulated CDK2 activity observed in *in vitro* assays, suggesting that CDK2 may be directly responsible for the *in vivo* phosphorylation of H1. H1 phosphorylation has been proposed to lead to a relaxation of chromatin structure due to a decreased affinity of this protein for chromatin after phosphorylation. In accord with this, chromatin from the $Rb^{-/-}$ cells is more susceptible to micrococcal nuclease digestion than that from $Rb^{+/+}$ fibroblasts. Increased H1 phosphorylation and relaxed chromatin structure have also been observed in cells expressing several oncogenes, suggesting a common mechanism in oncogene and tumor suppressor gene function.**

pRb, the product of the retinoblastoma susceptibility gene (*Rb*), is functionally inactivated late in the G_1 phase of the cell cycle, a step that is crucial for progression into S phase (1). This inactivation occurs as a consequence of the phosphorylation of pRb by cyclin-dependent kinases (CDKs) in association with their regulatory cyclin subunits (2–4). In particular, cyclin D/CDK4,6 complexes and cyclin E/CDK2 complexes, all of which are active late in G_1, have been shown to phosphorylate pRb in cells after their ectopic expression and *in vitro*. This phosphorylation of pRb late in G_1 prevents the protein from binding to various cellular transcription factors (1). Recently, it has been shown that cyclin D/CDK4,6 activity is not required in cells lacking pRb function (5–7), suggesting that the major function of these regulatory proteins is the phosphorylation of pRb.

In addition to serving as a substrate for cyclin/CDKs, pRb also regulates expression of cyclin E through transcriptional repression of the cyclin E promoter (8–10). Thus, we have observed that primary mouse embryo fibroblasts lacking a functional *Rb* gene display elevated cyclin E protein levels and CDK2 activities (9). This may explain the shortened G_1 of these mutant cells (9, 11), since the regulated expression of cyclin E is necessary for controlled G_1 progression (12, 13).

Another line of research has addressed changes in the phosphorylation state of the linker histone, H1, in this phase of the cell cycle. As cells progress into S phase, H1 becomes phosphorylated (14, 15). The protein remains in this state until undergoing additional extensive phosphorylation before mitosis. Some have proposed that H1 phosphorylation leads to a decondensation of chromatin structure due to a decreased affinity of this histone for chromatin (14). This is supported by the demonstration that cells expressing various oncogenes display increased H1 phosphorylation and an increase in the accessibility of chromatin to nuclease digestion (16, 17).

The identity of the G_1/S phase kinase responsible for H1 phosphorylation is unknown, although the major late G_1 CDK, CDK2, is one attractive candidate. Indeed, H1 is a good substrate for CDK2 phosphorylation *in vitro* but a poor one for the other G_1 CDKs, 4 and 6 (18). CDC2, the major G_2 CDK, has been implicated in the phosphorylation of H1 before mitosis (19). These various phosphorylation events have been proposed as necessary steps in providing chromatin access to those proteins responsible for S phase replication and M phase chromatin condensation (14).

We have examined the state of phosphorylation of H1 as it relates to (*i*) CDK2 activity, (*ii*) chromatin structure, and (*iii*) G_1 progression. These parameters were examined in WI38 human diploid lung fibroblasts and in the *Rb*-deficient cells which, as mentioned above, contain elevated cyclin E levels and CDK2 activities. Our data indicate that H1 is phosphorylated late in G_1 by CDK2 and that deregulation of this activity in $Rb^{-/-}$ fibroblasts leads to a relaxed chromatin structure in these cells.

MATERIALS AND METHODS

Cell Culture. Early passage WI38 human diploid lung fibroblasts were obtained from the American Type Culture Collection. They were maintained in Dulbecco's modified Eagle's medium (DMEM) plus 15% inactivated fetal bovine serum (FBS) and antibiotics and passaged after reaching confluency at 1:2 every 3 days. $Rb^{+/+}$ and $Rb^{-/-}$ primary mouse embryo fibroblasts were isolated from embryos at 12.5 days of gestation (20) and maintained in DMEM plus 15% inactivated FBS and antibiotics. These cells were used before passage eight, having been split 1:2 every 2–3 days. For cell synchronization experiments, WI38 cells and mouse embryo fibroblasts were maintained in DMEM lacking serum for 72 hr before readdition of inactivated FBS to 15%.

^{3}H-Thymidine Labeling of Cells. Cells (5×10^4) were plated in each well of a 24-well plate and grown to ≈90% confluency before serum starvation as described above. The cells were then labeled with 2 mCi/ml (1 Ci = 37 GBq) [^{3}H]thymidine in DMEM minus serum for 1 hr before the indicated times. They were then treated with 0.5 ml ice cold 5% trichloroacetic acid for 30 min on ice before extensive washing with H_2O, lysis with 0.5 M NaOH, and scintillation counting.

Immunoprecipitations and Kinase Assays. E1A lysis buffer was used to prepare cell lysates at the indicated times as described (21). Kinase assays were performed as described (21) using equal amounts of protein for each immunoprecipitation. Kinase substrates were either calf thymus histone H1 (see Figs. 1 and 2) or total histones (see Fig. 3) (Boehringer

The publication costs of this article were defrayed in part by page charge payment. This article must therefore be hereby marked "*advertisement*" in accordance with 18 U.S.C. §1734 solely to indicate this fact.

Abbreviations: CDK, cyclin-dependent kinase; FBS, fetal bovine serum; CPM, count(s) per minute.

‡To whom reprint requests should be addressed. e-mail weinberg@wi.mit.edu.

Mannheim). Antibodies to CDK2 were from Santa Cruz Biotechnology.

Immunoblot Analyses. For immunoblot analyses, mouse embryo fibroblasts were lysed with SDS/PAGE sample buffer before electrophoresis, transfer to nitrocellulose membranes, and protein detection according to standard procedures (22) and as described (9). Alternatively, histone H1 was partially purified by 5% perchloric acid extraction of WI38 cell nuclei before immunoblot analysis. Protein amounts were normalized by spectrophotometric methods and Ponceau S staining of the nitrocellulose filters. Antibodies to phosphorylated histone H1 were a gift from C. D. Allis (University of Rochester, Rochester, NY), whereas those to CDK2 were obtained from Santa Cruz Biotechnology.

Micrococcal Nuclease Digestions. Nuclei preparations for micrococcal nuclease digestions were performed as described (23). Nuclei were resuspended at 10^8 nuclei/ml. Digestions were performed at 375 units of micrococcal nuclease (Boehringer Mannheim) per ml at room temperature for the indicated times. For the experiment of Fig. 2*D*, the mouse embryo fibroblasts' nuclei were lysed with SDS after the indicated times of nuclease digestion. Electrophoresis of 5 μg of purified DNA was through 1% agarose gels.

For the experiment of Fig. 1*B*, nuclei were isolated from [^{3}H]thymidine-labeled, serum-starved WI38 cells restimulated with serum for the indicated times. After nuclease digestions for 10 min as described above, the nuclei were microcentrifuged and the supernatant was removed with care taken not to disturb the pellet. The count per minute (CPM) in the nuclei and supernatant was determined by scintillation counting and the percentage of total counts released into the supernatant is displayed.

Two-Dimensional Phosphopeptide Mapping. For the metabolically labeled samples, histone H1 was isolated by 5% perchloric acid extraction of $Rb^{-/-}$ cell nuclei labeled with [^{32}P]-orthophosphate for 4 hr. Labeling was from 12 to 16 hr after the addition of 15% inactivated FBS to starved cells. For the *in vitro* labeled samples, H1 was isolated from serum-starved $Rb^{-/-}$ cells as described above. Kinase reactions were as described (21) using baculovirus-produced cyclin E/CDK2 (a gift of Y. Sun, Whitehead Institute for Biomedical Research). Two-dimensional phosphopeptide mapping was performed as described (24).

RESULTS

Cell Cycle-Specific Changes in CDK2 Activity, Chromatin Structure, and Histone H1 Phosphorylation in WI38 Cells. To establish a correlation between G_1 progression, CDK2 activity, and H1 phosphorylation, we employed WI38 human diploid lung fibroblasts, which can be highly synchronized by serum starvation followed by readdition (25–27). In the experiments described here, WI38 cells were starved of serum for 72 hr before the readdition of serum to a final concentration of 15%. Fig. 1*A* shows the CDK2-associated kinase activity from lysates prepared at the indicated times after serum readdition. In addition, the timing of G_1 and S phase entry was analyzed by [^{3}H]thymidine incorporation and is shown in Fig. 1*B*. The *in vitro* H1 kinase activity of CDK2 increased 8 hr after serum readdition and continued to rise until peaking 20–24 hr after the addition of serum to starved cells (Fig. 1*A*); DNA synthesis began between 12 and 16 hr after serum readdition and peaked after 20 hr (Fig. 1*B*). Therefore, CDK2 activity began to rise in mid/late G_1 and peaked in S phase.

To gauge changes in chromatin structure associated with G_1 progression and S phase entry, the experiment of Fig. 1*B* was performed. [^{3}H]Thymidine-labeled, serum-starved WI38 cells were serum-stimulated for the indicated times before isolation of nuclei. The nuclei were subsequently incubated with micrococcal nuclease as described in *Materials and Methods*. After 10 min of digestion, the nuclei were pelleted and the amounts of DNA released into the supernatant and remaining in the pellet

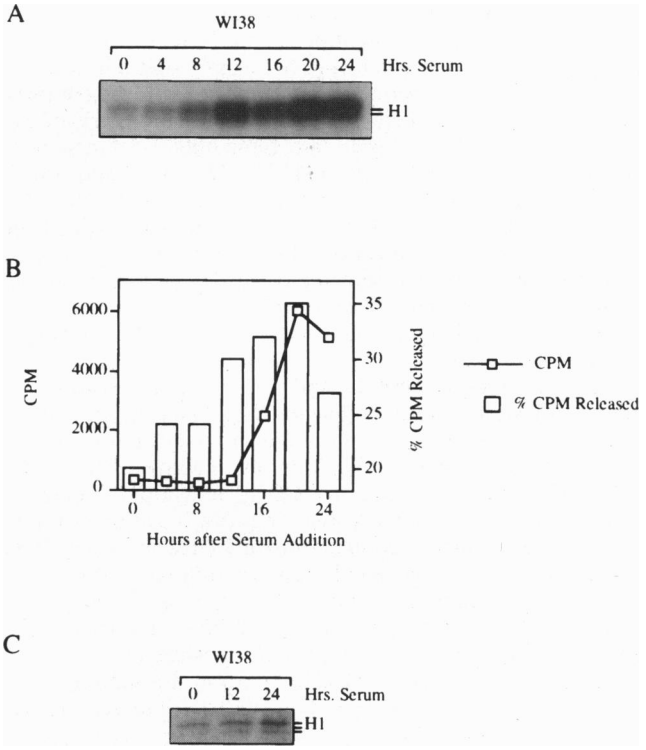

FIG. 1. Cell cycle analysis of CDK2 activation, chromatin structure, and histone H1 phosphorylation in WI38 fibroblasts. (*A*) CDK2 activation. Histone H1 kinase activity of anti-CDK2 immunoprecipitates prepared after the addition of DMEM plus 15% inactivated FBS to starved WI38 cells for 0, 6, 12, 18, or 24 hr as indicated. The position of histone H1 is indicated. (*B*) Cell cycle progression and chromatin structure. The left ordinate (CPM) represents the [^{3}H]thymidine incorporation of WI38 cells labeled for 1 hr after the readdition of serum to starved cells for 0, 6, 12, 18, or 24 hr as indicated. Total CPM are plotted. The right ordinate (% CPM released) represents the percent of total CPM released into the supernatant from [^{3}H]thymidine-labeled, micrococcal nuclease digested WI38 cell nuclei prepared after readdition of 15% inactivated FBS to starved cells for 0, 6, 12, 18, or 24 hr as indicated. (*C*) Intracellular histone H1 phosphorylation. Immunoblot analysis of protein samples prepared after the readdition of serum to starved WI38 cells. Blots contain partially purified histone H1 prepared from nuclei of cells stimulated with serum for 0, 12, or 24 hr as indicated. Phosphorylated histone H1 was detected by polyclonal rabbit antibodies. The position of histone H1 is indicated. Protein amounts were normalized by spectrophotometric methods and Ponceau S staining of the nitrocellulose filters.

determined by measuring radioactivity. The percentage of the total CPM released into the supernatant is shown in Fig. 1*B*. The amount of radioactivity released provides an index of susceptibility of the chromatin to nuclease digestion and thus the degree of chromatin decondensation.

As shown in Fig. 1*B*, there was a slight increase in chromatin accessibility as the cells exited G_0, which may be due to the general increase in transcription observed as cells enter G_1 (28, 29). The accessibility of the chromatin to nuclease digestion rose in mid-G_1 12 hr after serum readdition and continued to increase until peaking in S phase 20 hr after serum restimulation. The increased nuclease susceptibility of the WI38 chromatin in mid-G_1 and S phase corresponded temporally with the profile of CDK2 activity observed in Fig. 1*A*.

The phosphorylation state of H1 was examined by employing an antibody that recognizes preferentially the phosphorylated form of this protein (30) (Fig. 1*C*). H1 was partially purified by acid extraction of WI38 cell nuclei at the indicated times after serum readdition to starved cells. Immunoblot analysis of these extracted proteins showed that the amount of phosphorylated H1 increased moderately in mid/late G_1 after

12 hr of serum readdition with a further increase occurring after 24 hr of serum restimulation (Fig. 1*C*). While the increase in H1 phosphorylation after 24 hr of serum restimulation could be due to a small number of cells prematurely entering mitosis, we consider this unlikely because the stoichiometry of H1 phosphorylation occurring in late G_2 is only 3–5 times more than that observed in S phase (31, 32). Therefore, the contribution of H1 phosphorylated in G_2 to the total amount of H1 phosphorylation observed in Fig. 1*C* is minimal provided the degree of cell synchronization obtained in our experiments (Fig. 1*B*). We conclude that increased H1 phosphorylation, CDK2 activation, and relaxation of chromatin structure all occur in the mid/late G_1 and S phases of the cell cycle (Fig. 1 *A* and *B*).

Increased CDK2 Activity and Intracellular Histone H1 Phosphorylation in pRb-Deficient Fibroblasts. As mentioned above, we previously have shown that primary mouse embryo fibroblasts homozygous for a mutant, inactive allele of *Rb* display premature and excessive CDK2 activation in mid/late G_1 when compared with wild-type cells (9). It was therefore of interest to determine if deregulation of CDK2 activity in these cells led to a change in the phosphorylation state of H1. Fig. 2*A* shows the immunoprecipitated CDK2-associated H1 kinase activity from lysates of $Rb^{+/+}$ and $Rb^{-/-}$ mouse embryo fibroblasts prepared at the indicated times after serum stimulation of serum-starved cells. In addition, the timing of G_1 and S phase entry was analyzed by [^{3}H]thymidine incorporation and is shown in Fig. 2*C*.

As observed previously (9), CDK2 activity is deregulated in the *Rb* mutant cells in that it rises 6 hr prematurely (12 vs. 18 hr), peaks 6 hr prematurely (18 vs. 24 hr), and reaches levels of activation that are ≈2-fold greater than those seen in wild-type cells (Fig. 2*A*). DNA replication also starts (12 vs. 18 hr) and peaks (18 vs. 24 hr) prematurely in the $Rb^{-/-}$ cells (Fig. 2*C*). Thus, the observed changes in CDK2 activity accompany and perhaps cause the shorter G_1 observed in the $Rb^{-/-}$ cells (9, 11) (Fig. 2*C*).

Immunoblotting of lysates from wild-type mouse embryo fibroblasts using the anti-phosphorylated H1 antibody revealed a slight increase in the phosphorylation of one H1 isoform after 18 hr of serum restimulation in late G_1/S and a further increase 24 hr after serum readdition at the peak of S phase (Fig. 2 *B* and *C*). This isoform is most likely H1b, because the antibody has a strong preference for this particular isoform (30). This was similar to the pattern of H1 phosphorylation observed in WI38 cells (Fig. 1*C*). In contrast, the $Rb^{-/-}$ cells exhibited greatly elevated amounts of phosphorylated H1 in the G_0, G_1, and S phases of their cell cycle (Fig. 2*B*). The elevated levels of phosphorylated H1 in the serum-starved mutant cells were not a consequence of incomplete G_0 entry in these cells since the $Rb^{+/+}$ and $Rb^{-/-}$ cells arrest equally well after serum starvation (9) (Fig. 2*C* and data not shown). The levels of phosphorylated H1 in the mutant cells rose initially in late G_1/S after 12 hr of serum restimulation, and peaked after 18 hr. These kinetics of activation mirrored those of CDK2-associated H1 kinase activity observed *in vitro* (9) (Fig. 2*A*).

Relaxed Chromatin Structure in $Rb^{-/-}$ Fibroblasts. As mentioned, cells displaying increased levels of H1 phosphorylation have been found to contain a less condensed chromatin structure that is more accessible to nuclease digestion (16, 17). For this reason, it was of interest to compare the chromatin structure of the $Rb^{-/-}$ and $Rb^{+/+}$ cells. To this end, nuclei were isolated from both cell types, while in G_0 (following 72 hr of serum starvation) and G_1/S (12 hr after serum restimulation). The nuclei were then digested with micrococcal nuclease for increasing lengths of time before lysis and DNA purification. In this experiment, the degree of nuclease digestion was assessed by resolving the resulting purified DNA samples by electrophoresis on agarose gels.

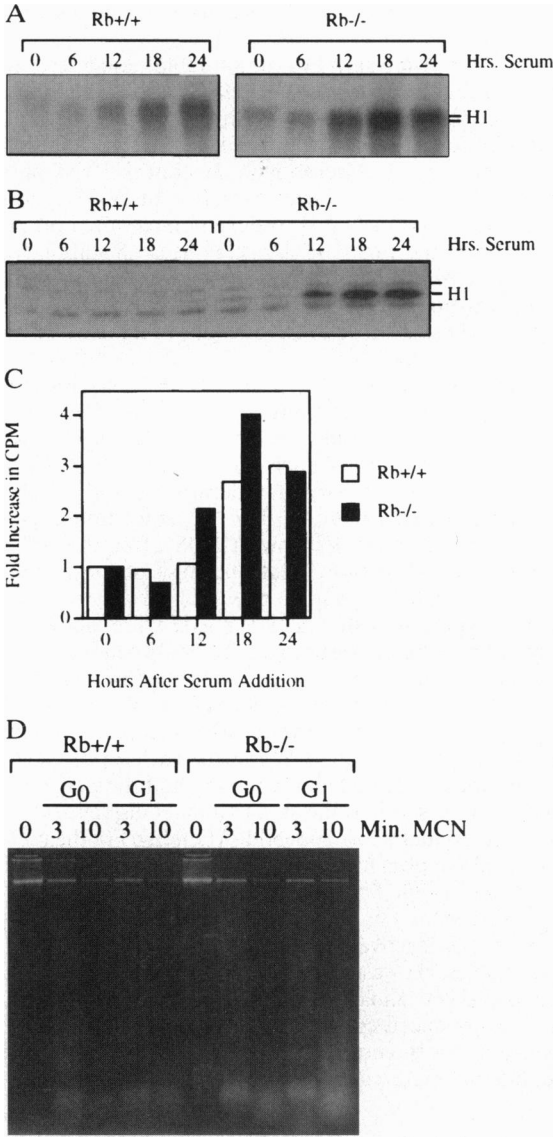

FIG. 2. Cell cycle analysis of CDK2 activation, chromatin structure, and histone H1 phosphorylation in $Rb^{+/+}$ and $Rb^{-/-}$ primary mouse embryo fibroblasts. (*A*) CDK2 activation. Histone H1 kinase activity of anti-CDK2 immunoprecipitates prepared after the addition of DMEM plus 15% inactivated FBS to starved $Rb^{+/+}$ and $Rb^{-/-}$ cells for 0, 6, 12, 18, or 24 hr as indicated. The position of histone H1 is indicated. (*B*) Intracellular histone H1 phosphorylation. Immunoblot analysis of protein samples prepared after the readdition of serum to starved $Rb^{+/+}$ and $Rb^{-/-}$ cells. Blots contain total protein lysates from cells stimulated with serum for 0, 6, 12, 18, or 24 hr as indicated. Phosphorylated histone H1 was detected by polyclonal rabbit antibodies. Protein amounts were normalized by spectrophotometric methods and Ponceau S staining of the nitrocellulose filters. The position of histone H1 is indicated. (*C*) Cell cycle analysis. [^{3}H]Thymidine incorporation of $Rb^{+/+}$ and $Rb^{-/-}$ cells labeled for 1 hr after the readdition of serum to starved cells for 0, 6, 12, 18, or 24 hr as indicated. The CPM from the unstimulated samples is arbitrarily defined as 1 and the fold increase in CPM in the subsequent samples is displayed as the *y* axis. (*D*) Micrococcal nuclease digestion of nuclei from $Rb^{+/+}$ and $Rb^{-/-}$ primary mouse embryo fibroblasts. Agarose gel electrophoresis of DNA isolated from nuclei of $Rb^{+/+}$ and $Rb^{-/-}$ cells that were digested with micrococcal nuclease for 0, 3, or 10 min as indicated before lysis. Nuclei were prepared from cells that were either serum starved (G_0) or restimulated for 12 hr (G_1) before isolation of nuclei. Equal amounts of DNA (5 μg) were loaded in each lane as determined by spectrophotometric methods.

Fig. 2*D* shows that the chromatin of the $Rb^{-/-}$ fibroblasts was more susceptible to micrococcal nuclease digestion both in

G_0 and G_1, with the difference becoming most evident as the $Rb^{-/-}$ cells progressed into S phase (Fig. 2*D*, lanes labeled G_1). This was evidenced by the dramatic relative increase in lower molecular weight DNA fragments in all of the samples derived from $Rb^{-/-}$ cells. Indeed, even in the absence of added nuclease (Fig. 2*D*, 0 min micrococcal nuclease), an increase in smaller DNA fragments was observed. This may be attributable to the activity of endogenous cellular nucleases, which were able to act on the relatively open chromatin of the $Rb^{-/-}$ cells.

Phosphorylation of Histone H1 by Cyclin E/CDK2. To determine if the pattern of H1 phosphorylation in G_1 was reflective of the biochemical activities of CDK2, we compared H1 phosphorylated *in vitro* by baculovirus-produced cyclin E and CDK2 to that phosphorylated intracellularly late in G1. We first wished to characterize our baculovirus-produced cyclin E/CDK2 complexes to assure that the *in vitro* phosphorylation of H1 was indeed due to the activity of these complexes and conversely not due to a contaminating insect kinase.

Fig. 3*A* examines the kinase activity and specificity of cyclin E/CDK2 produced by baculovirus expression in insect cells. Lysates from insect cells expressing cyclin E alone displayed H1 kinase activity, which increased upon CDK2 coexpression (Fig. 3*A*, right two lanes). However, the kinase activities of these lysates were not specific, as they phosphorylated the core histones as well as other proteins present in the total histone preparation (Fig. 3*A*, right two lanes). This non-specific kinase activity was dependent on the baculovirus expression of a cyclin or CDK in the insect cells and probably reflects the recruitment of insect cyclin and CDKs by the ectopically expressed human proteins (not shown). In contrast, anti-CDK2 immunoprecipitates from lysates of mock-infected or cyclin E virus-infected cells displayed a complete absence of kinase activity toward any protein in the total histone preparation (Fig. 3*A*, left two lanes). However, anti-CDK2 immunoprecipitates from lysates of cyclin E/CDK2 expressing cells displayed very high levels of H1 kinase activity and a total lack of activity toward other proteins in the histone preparation (Fig. 3*A*, middle lane).

This anti-CDK2 immunoprecipitate from lysates of cyclin E/CDK2 expressing insect cells was then used to phosphorylate murine H1 that had been partially purified from serum-starved $Rb^{-/-}$ primary fibroblasts. Two-dimensional phosphopeptide analysis of this *in vitro* phosphorylated H1 revealed a pattern consisting of nine ^{32}P-labeled spots of various intensities (Fig. 3*B*, *Top* and *Bottom*). Comparison of this pattern with that obtained from ^{32}P-labeled H1 from late G_1/S phase (labeling from 12 to 16 hr after serum restimulation of serum-starved cells) $Rb^{-/-}$ fibroblasts shows that the same nine spots were also phosphorylated intracellularly (Fig. 3*B*, *Middle* and *Bottom*). However, the relative intensities of several of the spots differed in the two samples. For example, spots 5 and 8 were relatively underphosphorylated and spot 2 was relatively hyperphosphorylated intracellularly as compared with *in vitro*. This may have been due to the relative differences in the stabilities of various phosphorylations in the cell, the relative *in vivo* contributions of both cyclin E/CDK2 and cyclin A/CDK2 to these phosphorylations, altered accessibility of CDK2 to H1 in chromatin, or to additional kinases unrelated to cyclin/CDK that are known to phosphorylate H1 (33). These results indicate that the modification of H1 observed in the late G_1 phase of mouse fibroblasts is very similar to that generated by cyclin E/CDK2 *in vitro*, indicating that this cyclin/CDK complex may indeed be responsible for the observed intracellular phosphorylation.

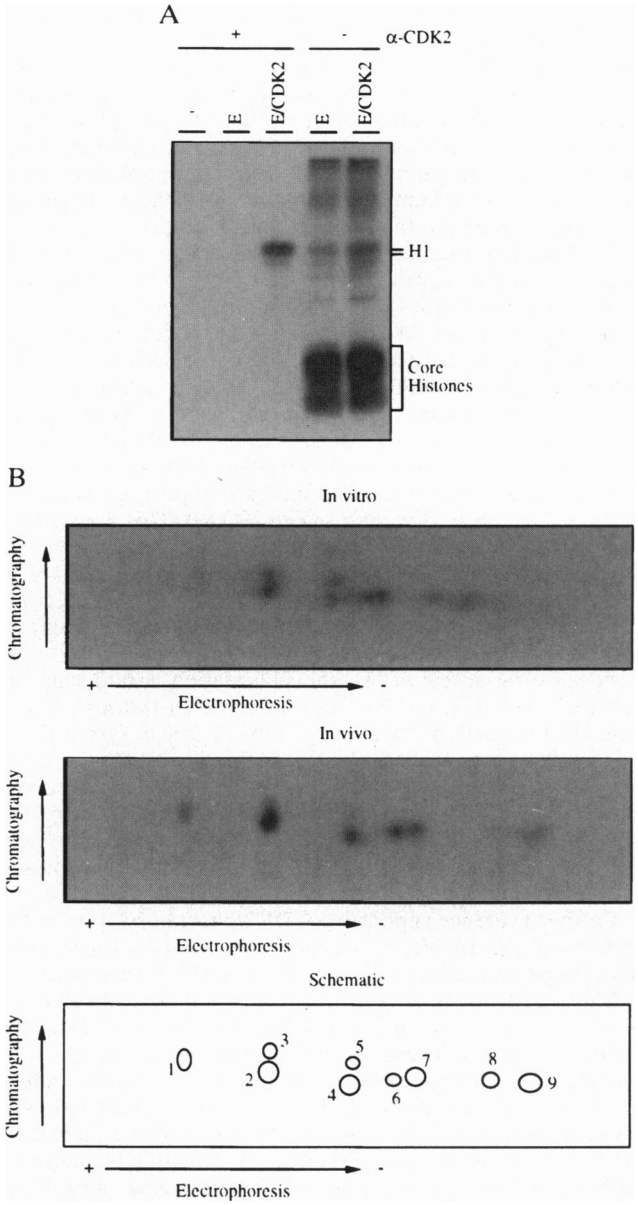

FIG. 3. Phosphopeptide analysis of histone H1 phosphorylated intracellularly and *in vitro*. (*A*) Characterization of baculovirus-produced cyclin E and CDK2. Lysates from SF9 insect cells containing either empty (−), cyclin E (E), or cyclin E and CDK2 (E/CDK2) expression vectors were used to phosphorylate a total histone preparation (Boehringer Mannheim). Insect cell lysates were either immunoprecipitated by an anti-CDK2 antibody before being used in the kinase assay (+ α-CDK2) or used without prior immunoprecipitation (− α-CDK2). The position of histone H1 and the core histones is indicated. (*B*) Two-dimensional phosphopeptide analysis of histone H1 phosphorylated intracellularly and *in vitro*. Histone H1 partially purified from serum starved $Rb^{-/-}$ cells was used as an *in vitro* substrate for complexes immunoprecipitated by anti-CDK2 antibodies from SF9 insect cells containing expression vectors for cyclin E and CDK2 (as in *A*). The two-dimensional radiolabeled phosphopeptide pattern obtained is shown (In vitro). Alternatively, H1 was partially purified from $Rb^{-/-}$ cells labeled with ^{32}P-orthophosphate after the readdition of serum to starved cells (labeling was from 12 to 16 hr after serum restimulation). The two-dimensional radiolabeled phosphopeptide pattern obtained is shown (In vivo). A schematic representation of the patterns obtained is presented as a reference (Schematic). The directions of electrophoresis and chromatography are shown. The apparent difference in the positions of some of the spots (8 and 9) in the two radiolabeled sample is due to the *in vivo* sample having run farther during electrophoresis.

DISCUSSION

Phosphorylation of H1 has been shown to be regulated during cell cycle progression (14, 15). Levels are lowest in G_1, increase as cells progress into S phase, and further increase at mitosis before dropping sharply after metaphase (32, 34, 35). Phos-

phorylation occurs at the N- and C- terminal arms of H1 at cdc2 phosphorylation consensus sequences, and indeed cdc2 has been shown to phosphorylate H1 prior to mitosis (19, 36). These sites are also phosphorylated by CDK2 *in vitro,* suggesting that it may be responsible for the H1 phosphorylation observed in G_1. We have shown a temporal correlation between CDK2 activation and intracellular H1 phosphorylation late in G_1 in WI38 human diploid lung fibroblasts, suggesting that these events are functionally linked (Fig. 1).

We have also examined the state of phosphorylation of H1 in $Rb^{+/+}$ and $Rb^{-/-}$ primary mouse embryo fibroblasts, since CDK2 kinase activities peak earlier and higher in the $Rb^{-/-}$ cells (Fig. 2*A*) (9). We find a profile of intracellular H1 phosphorylation that temporally mimics the activity of CDK2 observed *in vitro* in both cell types (Fig. 2*A* and *B*). In addition, the $Rb^{-/-}$ cells display highly elevated levels of H1 phosphorylation in the G_0, G_1, and S phases of their cell cycle with the peak levels being approximately 10-fold higher. This is substantially more than the 2-fold increase in peak CDK2 activities observed in *in vitro* assays (Fig. 2*A*) (9). This discrepancy may be due to the nature of the *in vitro* assay employed. Therefore, although strong conclusions can be made concerning the kinetics of CDK2 activation in living cells, we could obtain only qualitative measures of the levels of enzyme activity from these *in vitro* assays.

Because the levels of H1 phosphorylation vary during the cell cycle (14, 15), the increase observed in the $Rb^{-/-}$ cells could be the result of differences in the degree of synchrony of these cells compared with the $Rb^{+/+}$ fibroblasts. However, we were able to impose comparable degrees of synchrony on both cell types in all of our experiments (Fig. 2*C*) (9). Therefore, the observed differences in H1 phosphorylation in the $Rb^{+/+}$ and $Rb^{-/-}$ cells could not be attributed to substantial differences in the synchronization of these two cell populations.

Further evidence supporting CDK2 phosphorylation of H1 in late G_1 was obtained by comparing the two-dimensional phosphopeptide map of H1 phosphorylated *in vitro* by cyclin E/CDK2 and intracellularly late in G_1/S (Fig. 3). Both analyses display a pattern of nine radiolabeled spots, some of which differ in intensity. These variations could be due to relatively unstable H1 phosphorylations that occur late in G_1 before additional stable phosphorylation events in S phase (31, 32). Indeed, some have proposed that initially unstable phosphorylation events produce a chromatin conformation that permits replication initiation, whereas subsequent stable phosphorylation events occur following passage of replication forks (31, 32). It is tempting to speculate that the initial phosphorylation of H1 in late G_1 is by cyclin E/CDK2, whereas the ensuing modification is performed during S phase by cyclin A/CDK2.

We observed an opening of chromatin structure concomitant with CDK2 activation, H1 phosphorylation, and late G_1/S progression in WI38 cells (Fig. 1), suggesting that these events are functionally linked. This correlation was further strengthened by examination of the $Rb^{-/-}$ fibroblasts, which display a chromatin structure that is significantly more susceptible to nuclease digestion than that of wild-type cells (Fig. 2*D*). This was not a consequence of differences in cell cycle distribution, since the differences were observed both in cells that were in G_0 and in G_1/S. In addition, WI38 cells showed an opening of chromatin structure in late G_1, which accompanied the activation of CDK2 and preceded entrance into S phase (Fig. 1), suggesting that some degree of chromatin decondensation occurs independently of S phase entrance.

The precise role of H1 phosphorylation and its influence on chromatin structure remains controversial. H1 phosphorylation has been proposed to lead to chromosome condensation before mitosis (15). However, there are biological systems in which highly condensed chromatin is observed in the presence of dephosphorylated H1 (14). In addition, chromatin assembled *in vitro* with phosphorylated H1 exhibits a more open structure (37, 38). Hence, it has been proposed that H1 phosphorylation leads to a decondensation of chromatin as a prerequisite change that permits subsequent access to the chromatin template by factors involved directly in DNA replication, transcription, and mitotic chromosome condensation (14, 39). Indeed, simian virus 40 minichromosomes assembled with phosphorylated rather than unphosphorylated H1 are replicated with higher efficiency (38). Furthermore, cells expressing various oncogenes exhibit elevated levels of phosphorylated H1 (16, 17) and a relaxed chromatin structure (16, 17, 28, 29), further supporting a link between H1 phosphorylation and chromatin decondensation.

We and others have shown that cells lacking a functional *Rb* gene no longer require cyclin D/CDK4,6 activity for cell cycle progression (5–7), suggesting that the major function of cyclin D/CDK4,6 complexes is the phosphorylation of pRb. In addition, we have also shown that pRb is a repressor of cyclin E transcription (9, 10). Thus, the levels of cyclin E mRNA and protein rise dramatically in $Rb^{-/-}$ fibroblasts independent of cell cycle position and in $Rb^{+/+}$ cells late in G_1 after pRb phosphorylation and inactivation (9). This in turn contributes to increased CDK2 activity and S phase entry. We provide evidence here that this increase in CDK2 activity results in phosphorylation of H1 and that this leads to an opening of the chromatin template critical for the initiation of DNA replication. Taken together with previous results, our data suggest a progression of molecular events in G_1 leading from cyclin D/CDK4,6 activation to S phase initiation.

We would like to thank C. David Allis for the generous gift of antibodies directed against phosphorylated histone H1 and Yin Sun for baculovirus-produced cyclin E and CDK2. Comments on the manuscript by Peter Becker, Raphael Sandaltzopoulos and Rene Medema are greatly appreciated. R.E.H. was supported by the Cancer Research Foundation of America. This work was supported by a grant from the American Cancer Society to R.A.W. R.A.W. is an American Cancer Society Research Professor.

1. Weinberg, R. A. (1995) *Cell* **81,** 323–330.
2. Hinds, P. W., Mittnacht, S., Dulic, V., Arnold, A., Reed, S. I. & Weinberg, R. A. (1992) *Cell* **70,** 993–1006.
3. Kato, J., Matsushime, H., Hiebert, S. W., Ewen, M. E. & Sherr, C. J. (1993) *Genes Dev.* **7,** 331–342.
4. Ewen, M. E., Sluss, H. K., Sherr, C. J., Matsushime, H., Kato, J. & Livingston, D. M. (1993) *Cell* **73,** 487–497.
5. Medema, R. H., Herrera, R. E., Lam, F. & Weinberg, R. A. (1995) *Proc. Natl. Acad. Sci. USA* **92,** 6289–6293.
6. Lukas, J., Parry, D., Aagaard, L., Mann, D. J., Bartkova, J., Strauss, M., Peters, G. & Bartek, J. (1995) *Nature (London)* **375,** 503–506.
7. Koh, J., Enders, G. H., Dynlacht, B. D. & Harlow, E. (1995) *Nature (London)* **375,** 506–509.
8. DeGregori, J., Leone, G., Ohtani, K., Miron, A. & Nevins, J. R. (1995) *Genes Dev.* **9,** 2873–2887.
9. Herrera, R. E., Sah, V. P., Williams, B. O., Mäkelä, T. P., Weinberg, R. A. & Jacks, T. (1996) *Mol. Cell. Biol.* **16,** 2402–2407.
10. Geng, Y., Eaton, E. N., Picón, M., Roberts, J. M., Lundberg, A. S., Gifford, A., Sardet, C. & Weinberg, R. A. (1996) *Oncogene* **12,** 1173–1180.
11. Lukas, J., Bartkova, J., Rohde, M., Strauss, M. & Bartek, J. (1995) *Mol. Cell. Biol.* **15,** 2600–2611.
12. Tsai, L. H., Lees, E., Faha, B., Harlow, E. & Riabowol, K. (1993) *Oncogene* **8,** 1593–1602.
13. Koff, A., Giordano, A., Desai, D., Yamashita, K., Harper, J. W., Elledge, S., Nishimoto, T., Morgan, D. O., Franza, B. R. & Roberts, J. M. (1992) *Science* **257,** 1689–1694.
14. Roth, S. Y. & Allis, C. D. (1992) *Trends Biochem. Sci.* **17,** 93–98.
15. Bradbury, E. M. (1992) *BioEssays* **14,** 9–16.
16. Chadee, D. N., Taylor, W. R., Hurta, R. A., Allis, C. D., Wright, J. A. & Davie, J. R. (1995) *J. Biol. Chem.* **270,** 20098–20105.
17. Taylor, W. R., Chadee, D. N., Allis, C. D., Wright, J. A. & Davie, J. R. (1995) *FEBS Lett.* **377,** 51–53.

18. Matsushime, H., Quelle, D. E., Shurtleff, S. A., Shibuya, M., Sherr, C. J. & Kato, J. Y. (1994) *Mol. Cell. Biol.* **14,** 2066–2076.
19. Langan, T. A., Gautier, J., Lohka, M., Hollingsworth, R., Moreno, S., Nurse, P., Maller, J. & Sclafani, R. A. (1989) *Mol. Cell. Biol.* **9,** 3860–3868.
20. Jacks, T., Fazeli, A., Schmitt, E. M., Bronson, R. T., Goodell, M. A. & Weinberg, R. A. (1992) *Nature (London)* **359,** 295–300.
21. Makela, T. P., Tassan, J. P., Nigg, E. A., Frutiger, S., Hughes, G. J. & Weinberg, R. A. (1994) *Nature (London)* **371,** 254–257.
22. Ausubel, F. M., Brent, R., Kingston, R. E., Moore, D. D., Seidman, J. G., Smith, J. A. & Struhl, K. (1993) *Current Protocols in Molecular Biology* (Greene/Wiley, New York).
23. Reik, A., Schutz, G. & Stewart, A. F. (1991) *EMBO J.* **10,** 2569–2576.
24. Chen, F. & Weinberg, R. A. (1995) *Proc. Natl. Acad. Sci. USA* **92,** 1565–1569.
25. Coppock, D. L., Kopman, C., Scandalis, S. & Gilleran, S. (1993) *Cell Growth Differ.* **4,** 483–493.
26. Gope, M. L., Chun, M. & Gope, R. (1991) *Mol. Cell. Biochem.* **107,** 55–63.
27. Tupper, J. T., Kaufman, L. & Bodine, P. V. (1980) *J. Cell. Physiol.* **104,** 97–103.
28. Laitinen, J., Sistonen, L., Alitalo, K. & Holtta, E. (1995) *J. Cell. Biochem.* **57,** 1–11.
29. Laitinen, J., Sistonen, L., Alitalo, K. & Holtta, E. (1990) *J. Cell Biol.* **111,** 9–17.
30. Lu, M. J., Dadd, C. A., Mizzen, C. A., Perry, C. A., McLachlan, D. R., Annunziato, A. T. & Allis, C. D. (1994) *Chromosoma* **103,** 111–121.
31. Ajiro, K., Borun, T. W., Shulman, S. D., McFadden, G. M. & Cohen, L. H. (1981) *Biochemistry* **20,** 1454–1464.
32. Ajiro, K., Borun, T. W. & Cohen, L. H. (1981) *Biochemistry* **20,** 1445–1454.
33. van Holde, K. E. (1988) *Chromatin* (Springer, New York).
34. Gurley, L. R., Walters, R. A. & Tobey, R. A. (1975) *J. Biol. Chem.* **250,** 3936–3944.
35. Bradbury, E. M., Inglis, R. J. & Matthews, H. R. (1974) *Nature (London)* **247,** 257–261.
36. Norbury, C. & Nurse, P. (1992) *Annu. Rev. Biochem.* **61,** 441–470.
37. Kaplan, L. J., Bauer, R., Morrison, E., Langan, T. A. & Fasman, G. D. (1984) *J. Biol. Chem.* **259,** 8777–8785.
38. Halmer, L. & Gruss, C. (1996) *Nucleic Acids Res.* **24,** 1420–1427.
39. Lu, M. J., Mpoke, S. S., Dadd, C. A. & Allis, C. D. (1995) *Mol. Biol. Cell* **6,** 1077–1087.